Superfluidity of dipolar excitons in a transition metal dichalcogenide double layer

Oleg L. Berman and Roman Ya. Kezerashvili

Phys. Rev. B **96**, 094502 — Published 5 September 2017

DOI: 10.1103/PhysRevB.96.094502

Towards superfluidity of dipolar excitons in a TMDC double layer

Oleg L. Berman[1,2] and Roman Ya. Kezerashvili[1,2]
[1] *Physics Department, New York City College of Technology, The City University of New York, Brooklyn, NY 11201, USA*
[2] *The Graduate School and University Center, The City University of New York, New York, NY 10016, USA*
(Dated: July 21, 2017)

We study formation and superfluidity of dipolar excitons in double layer heterostructures formed by two transition metal dichalcogenide (TMDC) atomically thin layers. Considering screening effects for an electron-hole interaction via the harmonic oscillator approximation for the Keldysh potential, the analytical expressions for the exciton energy spectrum and the mean field critical temperature T_c for the superfluidity are obtained. It is shown that binding energies of A excitons are larger than for B excitons. The mean field critical temperature for a two-component dilute exciton system in a TMDC double layer is analyzed and shown that latter is an increasing function of the factor Q, determined by the effective masses of A and B excitons and their reduced mass. Comparison of the calculations for T_c performed by employing the Coulomb and Keldysh interactions demonstrates the importance of screening effects in TMDC.

PACS numbers: 71.20.Be, 71.35.-y, 71.35.Lk

I. INTRODUCTION

When a sufficient amount of bosons at low temperatures spontaneously occupy the single lowest energy quantum state, Bose–Einstein condensation (BEC) happens. The system of interacting bosons can experience the superfluidity, caused by BEC, analogously to the superfluid helium[1]. A BEC of weakly interacting particles was achieved experimentally in dilute gases of alkali atoms. This atomic BEC can be created at the nanokelvin temperatures, which are technically challenging to achieve. The progress in the experimental and theoretical research of the BEC of dilute supercold alkali gases is reviewed in Ref.[2].

The BEC for two-dimensional (2D) bosons with higher mass occurs at the temperatures greater than for bosons with lower mass, because the de Broglie wavelength for 2D system is inversely proportional to the square root of the mass of a particle. Therefore, BEC exists at much higher temperatures in a Bose gas of small mass particles, than in a system of relatively heavy alkali atoms. The small mass boson quasiparticles can be formed due to absorption of a photon by a semiconductor. Absorption of a photon leads to creation of an electron in a conduction band and a positive charge "hole" in a valence band. This electron-hole pair can form a bound state called an "exciton". The BEC and superfluid of such excitons are expected to exist at experimentally observed exciton densities at temperatures much higher than for the BEC of alkali atoms[3]. The BEC and superfluidity of dipolar (indirect) excitons, formed by electrons and holes, spatially separated in two parallel two-dimensional semiconductor quantum wells, were proposed[4]. The experimental observation of superfluidity of dipolar excitons in GaAs quantum wells was claimed recently[5]. The recent progress in experimental and theoretical studies of BEC of dipolar excitons in semiconductor quantum wells was reviewed[3,6–8].

Due to relatively large exciton binding energies in novel 2D semiconductors, such as transition metal dichalcogenides (TMDC), the BEC and superfluidity of dipolar excitons in double layers of TMDC can occur. Monolayers of TMDC such as MoS_2, $MoSe_2$, $MoTe_2$, WS_2, WSe_2, and WTe_2 are 2D semiconductors, belonging to a class of monolayer direct bandgap materials, attract an interest due various applications in electronics and opto-electronics[9]. Since contrary to gapless graphene, TMDC monolayers have the direct gap in a single-particle spectrum exhibiting the semiconducting band structure[10–13], excitons in TMDCs can be created by the laser pumping. The ground and excited states of direct excitons in mono- and few-layer TMDCs on a SiO_2 substrate were experimentally and theoretically studied[14]. Two distinct types of excitons in TMDC layers, labeled A and B, are formed due to significant spin-orbit splitting in the valence band[15]. The excitons of type A are created by spin-up electrons from conduction and spin-down holes from valence bands. The excitons of type B are created by spin-down electrons from conduction and spin-up holes from valence bands. While the spin-orbit splitting in the valence band is much larger than in the conduction band, in the valence band the energy for spin-down electrons is larger than for spin-up electrons. The spin-orbit spitting results in the experimentally observed energy difference between the A and B excitons[9]. Therefore, A and B excitons form a two-component Bose gas in TMDCs. Let us mention that caused by the lack of inversion symmetry in TMDC monolayers, spin-orbit splitting of energy bands generally occurs over the entire Brillouin zone[16,17]. Due to the Kramers theorem, the bands are doubly degenerate at the time-reversal invariant points Γ and M and at special k points along the Γ-M direction in the crystal momentum space, which are protected by crystal mirror symmetry[17]. In

TMDC monolayers, the low-energy bands at K± points at the centers of the valleys in the crystal momentum space are not spin degenerate[16,17].

High-temperature superfluidity can be observed for dipolar excitons in a heterostructure of two TMDC monolayers, separated by a hexagonal boron nitride (h-BN) insulating barrier[18]. The dipolar excitons were observed in heterostructures formed by monolayers of MoS_2 and $MoSe_2$ on a $Si-SiO_2$ substrate[19] and by monolayers of MoS_2 on a substrate constrained by hexagonal boron nitride layers[20]. The theoretical study of the phase diagram of 2D dipolar exciton condensates in a TMDC double layer was performed[21]. The high-temperature superfluidity of the two component Bose gas of A and B dipolar excitons in a transition metal dichalcogenide double layer was predicted in Ref.[22].

In this paper, we study the superfluidity of two-component dilute Bose gas of dipolar A and B excitons in different TMDC double layers. We search the candidates for higher temperature of superfluidity by comparing the results of the calculations for various TMDC double layers, formed by two monolayers of the same TMDC material and two different TMDC monolayers, when the transition metal atom is replaced by the other transition metal atom (e.g. for a MoS_2/WS_2 heterostructure) or when the chalcogenide atoms are replaced by the other chalcogenide atoms (e.g. for a $MoS_2/MoSe_2$ heterostructure). While an electron and a hole interact via the Coulomb potential, in general, affected by screening effects the electron-hole interaction in TMDC materials is described by the Keldysh potential [15]. In the framework of the harmonic oscillator approximation for the electron-hole interaction in TMDC double layer heterostructure we obtain the analytical expressions for the exciton energy spectrum and the mean field critical temperature of superfluidity. The calculations are performed for both the Keldysh and Coulomb potentials, describing the interactions between the charge carriers, which allows to study the influence of the screening effects on the properties of a weakly interacting Bose gas of dipolar excitons in a TMDC double layer. Due to spin-orbit splitting around the K point in the Brillouin zone, the critical temperature T_c of superfluidity for a two-component exciton system in a TMDC double layer is higher than T_c for an exciton system in semiconductor (GaAs/AlGaAs) coupled quantum wells, where the spin degeneracy for the charge carriers occurs.

The paper is organized in the following way. In Sec. II, the two-body problem for an electron and a hole, spatially separated in two parallel TMDC monolayers, is formulated, and the energy spectrum, wave functions, and binding energies for a single dipolar exciton in a TMDC double layer are obtained. The exciton-exciton interaction is analyzed in Sec. III. In Sec. IV, the mean field critical temperature of superfluidity for the two-component dilute system of dipolar excitons in a TMDC double layer is obtained and analyzed. The conclusions follow in Sec. V.

II. TWO-BODY PROBLEM FOR AN ELECTRON AND A HOLE, SPATIALLY SEPARATED IN TWO PARALLEL TMDC MONOLAYERS

We consider electrons to be confined in a 2D TMDC monolayer, while an equal number of positive holes are placed in a parallel TMDC monolayer at a distance D away. The system of the charge carriers in two parallel TMDC layers is treated as a 2D system without interlayer hopping. The electron and hole via electromagnetic interaction $V(r_{eh})$, where r_{eh} is a distance between the electron and hole, could form a bound state, i.e., a dipolar exciton. The electron-hole recombination due to the tunneling of electrons and holes between different TMDC monolayers is suppressed by the dielectric barrier with the dielectric constant ε_d that separates two TMDC monolayers[22]. Therefore, the dipolar excitons, formed by electrons and holes, located in two different parallel TMDC monolayers, have a longer lifetime than the direct excitons. After projection the electron position vector onto the TMDC plane with holes and replacing the relative coordinate vector $\mathbf{r}_{eh}$ by its projection $\mathbf{r}$ on this plane and taking into account that $r_{eh}=\sqrt{r^2+D^2}$, the potential $V(r_{eh})$ can be expressed as $V(r)=V(\sqrt{r^2+D^2})$, where r is the relative distance between the hole and the projection of the electron position onto the TMDC monolayer with holes. Thus, a dipolar exciton can be described by a two-body 2D Schrödinger equation with potential $V(\sqrt{r^2+D^2})$, employing in-plane coordinates $\mathbf{r}_1$ and $\mathbf{r}_2$ for the hole and the projection of the electron, respectively, so that $\mathbf{r}=\mathbf{r}_1-\mathbf{r}_2$.

The Hamiltonian of an electron and a hole, spatially separated in two parallel TMDC monolayers with the interlayer distance D has the following form

$$\hat{H}_{ex}=-\frac{\hbar^2}{2m_e}\Delta_{\mathbf{r}_1}-\frac{\hbar^2}{2m_h}\Delta_{\mathbf{r}_2}+V(r), \tag{1}$$

where $\Delta_{\mathbf{r}_1}$ and $\Delta_{\mathbf{r}_2}$ are the Laplacian operators with respect to the components of the vectors $\mathbf{r}_1$ and $\mathbf{r}_2$, respectively, and m_e and m_h are the effective masses of the electron and hole, respectively. The problem of the in-plane motion of interacting electron and hole forming the exciton in a TMDC double layer can be reduced to that of one particle with the reduced mass $\mu=m_e m_h/\left(m_e+m_h\right)$ in a $V(r)$ potential and motion of the center-of-mass of the exciton with the mass $M=m_e+m_h$. Following the standard procedure for the two-body problem[23], we introduce the coordinates of the center-of-mass $\mathbf{R}$ of an exciton and the coordinate of the relative motion $\mathbf{r}$ of an electron and hole

as $\mathbf{R} = (m_e\mathbf{r}_1 + m_h\mathbf{r}_2)/(m_e + m_h)$ and $\mathbf{r} = \mathbf{r}_1 - \mathbf{r}_2$, correspondingly. The Hamiltonian $\hat{H}_{ex}$ can be represented in the form: $\hat{H}_{ex} = \hat{H}_R + \hat{H}_r$, where the Hamiltonians of the motion of the center-of-mass $\hat{H}_R$ and relative motion of electron and a hole $\hat{H}_r$.

The solution of the Schrödinger equation for the center-of-mass of an exciton $\hat{H}_R\psi(\mathbf{R}) = \mathcal{E}\psi(\mathbf{R})$ is the plane wave $\psi(\mathbf{R}) = e^{i\mathbf{PR}/\hbar}$ with the quadratic energy spectrum $\mathcal{E} = P^2/(2M)$, where $\mathbf{P}$ is the momentum of the center-of-mass of an exciton.

A. The harmonic oscillator approximation of Keldysh potential for a TMDC double layer

In TMDC layers due to the screening effects[15,24–27] the electron-hole attraction has to be described by the Keldysh potential[28,29]. We assume the following form of the Keldysh potential[30]:

$$V(r_{eh}) = -\frac{\pi k e^2}{(\varepsilon_1 + \varepsilon_2)\,\rho_0}\left[H_0\left(\frac{r_{eh}}{\rho_0}\right) - Y_0\left(\frac{r_{eh}}{\rho_0}\right)\right], \tag{2}$$

where $k = 9 \times 10^9\ N \times m^2/C^2$, $H_0(x)$ and $Y_0(x)$ are Struve and Bessel functions of the second kind of order $\nu = 0$, correspondingly, ε_1 and ε_2 are the dielectric constants of the dielectrics, surrounding the TMDC layer, ρ_0 is the screening length, defined by $\rho_0 = 2\pi\zeta/\left[(\varepsilon_1 + \varepsilon_2)/2\right]$, where ζ is the 2D polarizability. If the electron-hole separation is large, implying $r_{eh} \gg \rho_0$, the potential, given by Eq. (2), has the three-dimensional Coulomb tail, while for small electron-hole distances at $r_{eh} \ll \rho_0$ it turns to a logarithmic Coulomb potential for two 2D point charges. Throughout of this paper we assume that TMDC monolayers are embedded in the same material with dielectric constant ε_d and, therefore, we set $\varepsilon_1 = \varepsilon_2 = \varepsilon_d$.

Substituting $r_{eh} = \sqrt{r^2 + D^2}$ into Eq. (2), assuming $r \ll D$, and expanding Eq. (2) in Taylor series we obtain in the first order with respect to $(r/D)^2$:

$$V(r) = -V_0 + \gamma r^2, \tag{3}$$

where

$$V_0 = \frac{\pi k e^2}{2\varepsilon_d \rho_0}\left[H_0\left(\frac{D}{\rho_0}\right) - Y_0\left(\frac{D}{\rho_0}\right)\right], \tag{4}$$

$$\gamma = -\frac{\pi k e^2}{4\varepsilon_d \rho_0^2 D}\left[H_{-1}\left(\frac{D}{\rho_0}\right) - Y_{-1}\left(\frac{D}{\rho_0}\right)\right]. \tag{5}$$

If we use the Coulomb potential, the potential energy of the electron-hole attraction $V(r)$ is

$$V(r) = -\frac{k e^2}{\varepsilon_d\sqrt{r^2 + D^2}}. \tag{6}$$

Assuming $r \ll D$, we approximate $V(r)$ by the first two terms of the Taylor series and obtain

$$V(r) = -V_0 + \gamma r^2, \quad \text{where } V_0 = \frac{k e^2}{\varepsilon_d D}, \qquad \gamma = \frac{k e^2}{2\varepsilon_d D^3}. \tag{7}$$

The Keldysh potential and the harmonic oscillator approximation for the Keldysh potential for electron-hole attraction in a TMDC double layer, describing the electron-hole interaction in a TMDC double layer, given by Eqs. (2) and (3), respectively, are shown in Fig. 1. According to Figs. 1a and 1b, the difference between the potentials for different TMDC materials decreases as r increases. As seen from Fig. 1c, the harmonic oscillator approximation of the Keldysh potential is very much close to the exact Keldysh potential for small r, while it becomes larger than the exact Keldysh potential when r increases. Let us mention that indirect excitons were observed in two different MoS_2 layers separated by h-BN monolayers and surrounded by h-BN cladding layers, since h-BN monolayers are characterized by relatively small density of the defects of their crystal structure[20]. Therefore, in our calculations we consider the TMDC monolayers to be separated by h-BN insulating layers. Besides we assume h-BN insulating layers to be located on the top and on the bottom of the TMDC double layer. In this case, $\varepsilon_d = 4.89$ is the effective dielectric constant, defined as $\varepsilon_d = \sqrt{\varepsilon^{\perp}}\sqrt{\varepsilon^{\parallel}}$[18], where $\varepsilon^{\perp} = 6.71$ and $\varepsilon^{\parallel} = 3.56$ are the components of the dielectric tensor for h-BN[31]. Throughout of this paper we consider the separation between two layers of TMDC materials in steps of $D_{hBN} = 0.333$ nm, corresponding to the thickness of one h-BN monolayer[18]. Therefore, the interlayer separation D is presented as $D = N_L D_{hBN}$, where N_L is the number of h-BN monolayers, placed between two TMDC monolayers. In Fig. 1 the number $N_L = 10$ of h-BN monolayers, located between two TMDC monolayers corresponds to $D = 3.33$ nm.

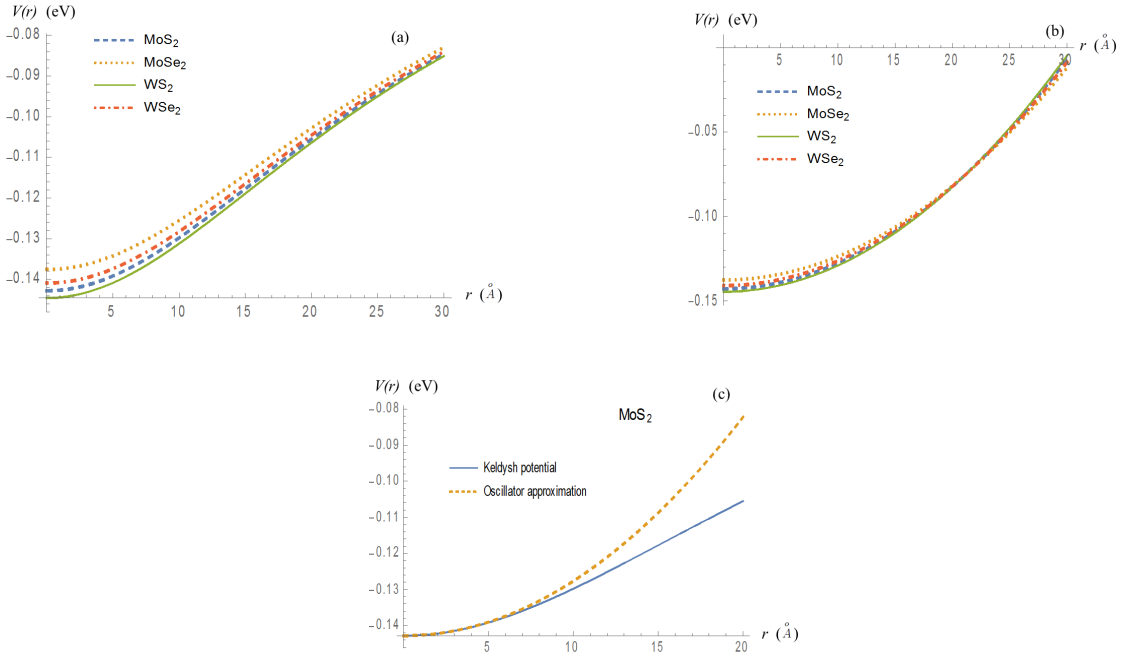

FIG. 1: (Color online) (a) The Keldysh potential for electron-hole attraction in different TMDC double layers, given by Eq. (2). (b) The harmonic oscillator approximation for the Keldysh potential for electron-hole attraction in different TMDC double layers, given by Eq. (3). (c) Comparison of the Keldysh potential and the Keldysh potential, approximated by the harmonic oscillator potential in a MoS_2 double layer. The calculations were performed for the number $N_L = 10$ of h-BN monolayers, located between two TMDC monolayers. The polarizabilities for TMDC materials are taken from Ref.[15].

B. The dipolar exciton energy spectrum and wave functions

The solution of the Schrödinger equation for the relative motion of an electron and a hole $\hat{H}_r\Psi(\mathbf{r}) = E\Psi(\mathbf{r})$ with the potential (3) is reduced to the problem of a 2D harmonic oscillator with the exciton reduced mass μ. The eigenfunctions and eigenenergy for a single particle in the parabolic well were first determined by Fock in 1928[32], later in Ref. [33], and was studied in detail in Ref.[34]. The single-particle eigenfunction for the two-dimensional oscillator was widely used for the description of a quantum dot[35].

Following Refs. [35,36] one obtains the radial Schrödinger equation and the solution for the eigenfunctions for the relative motion of an electron and a hole in a TMDC double layer in terms of associated Laguerre polynomials can be written as

$$\Psi_{NL}(\mathbf{r}) = \frac{N!}{a^{|L|+1}\sqrt{\widetilde{n}!\widetilde{n}'!}} 2^{-|L|/2}\mathrm{sgn}(L)^L r^{|L|} e^{-r^2/(4a^2)} \times L_N^{|L|}(r^2/(2a^2)) \frac{e^{-iL\phi}}{(2\pi)^{1/2}}, \tag{8}$$

where $N = \min(\widetilde{n}, \widetilde{n}')$, $L = \widetilde{n} - \widetilde{n}'$, $\widetilde{n}$, $\widetilde{n}' = 0, 1, 2, 3, \ldots$ are the quantum numbers, ϕ is the polar angle, and $a = \left[\hbar/\left(2\sqrt{2\mu\gamma}\right)\right]^{1/2}$.

The corresponding energy spectrum is given by

$$E_{NL} \equiv E_{e(h)} = -V_0 + (2N + 1 + |L|)\hbar\left(\frac{2\gamma}{\mu}\right)^{1/2}. \tag{9}$$

At the lowest quantum state $N = L = 0$ as it follows from Eq. (9) the ground state energy for the exciton is given by

$$E_{00} = -V_0 + \hbar\left(\frac{2\gamma}{\mu}\right)^{1/2}. \tag{10}$$

The important characteristics of the exciton is the square of the in-plane gyration radius r_X^2. It allows to estimate the condition when the excitonic gas is dilute enough. One can obtain the square of the in-plane gyration radius r_X of

TABLE I: Masses of excitons and D_0 for different TMDC materials. m_0 is an electron mass.

Exciton		MoS_2	$MoSe_2$	WS_2	WSe_2
A	Mass/m_0	1.1	1.33	0.84	0.93
	D_0, Å	0.29	0.23	0.32	0.30
B	Mass/m_0	0.98	1.15	0.62	0.66
	D_0, Å	0.31	0.25	0.37	0.36

a dipolar exciton[18], which is the average squared projection of an electron-hole separation onto the plane of a TMDC monolayer as

$$r_X^2 \equiv \left\langle r^2 \right\rangle = \int \Psi_{00}^*(\mathbf{r}) r^2 \Psi_{00}(\mathbf{r}) d^2 r = \frac{2\pi}{2\pi a^2} \int_0^{+\infty} r^2 e^{-\frac{r^2}{2a^2}} r dr = 2a^2. \tag{11}$$

Let us mention that the Taylor expansion of the electron-hole attraction potential in the first order with respect to r^2/D^2, presented by Eq. (3) is valid if $r_X^2 = 2a^2 \ll D^2$. Thus, one obtains that $\hbar/\sqrt{2\mu\gamma} \ll D^2$. The latter inequality holds for $D \gg D_0$. The value of D_0 depends on the effective masses of the electron and hole. For the Keldysh potential D_0 can be obtained from solution of the following transcendental equation:

$$D_0^3 = -\frac{2\hbar^2 \varepsilon_d \rho_0^2}{\pi k e^2 \mu \left[H_{-1}\left(\frac{D_0}{\rho_0}\right) - Y_{-1}\left(\frac{D_0}{\rho_0}\right) \right]}. \tag{12}$$

The following inequality should hold for the Keldysh potential:

$$-\frac{2\hbar^2 \varepsilon_d \rho_0^2}{\pi k e^2 \mu \left[H_{-1}\left(\frac{D}{\rho_0}\right) - Y_{-1}\left(\frac{D}{\rho_0}\right) \right]} \ll D^3. \tag{13}$$

For the Coulomb potential, we have $D_0 = \hbar^2 \varepsilon_d / \left(k e^2 \mu\right)$. The comparison of the latter expression for D_0 with Eq. (12) shows that in the case of the Keldysh potential D_0 depends on the screening length which is contingent on the 2D polarizability of TMDC material.

To estimate the condition of validity of the Taylor expansion we find D_0 by solving Eq. (12). The masses of dipolar excitons and D_0 for different TMDC materials are represented in Table I. The smallest D_0 corresponds to a $MoSe_2$ double layer, while largest D_0 corresponds to a WS_2 double layer. The values of D_0 are smaller for A dipolar excitons than for B dipolar excitons for the same TMDC double layers. Consideration of the double layer heterostructure that consists from two different TMDC layers, when in one of the layers the transition metal atom is replaced by the other transition metal atom (e.g. for a MoS_2/WS_2 heterostructure) or the chalcogenide atoms are replaced by the other chalcogenide atoms (e.g. for a $MoS_2/MoSe_2$ heterostructure) changes the value of D_0 insignificantly.

The binding energy of an exciton depends on the effective masses of an electron and a hole that constitute the A and B excitons and the polarizability of TMDC material. In our calculations throughout of this paper we use the set of effective masses for electrons and holes from Refs.[37,38] and the polarizability from Ref.[15]. The effective masses for the charge carriers in Refs.[37,38] and the polarizability in Ref.[15] were obtained by employing density functional theory (DFT) calculations. Let us mention that we consider the excitons, formed by the carriers at the K point in the crystal momentum space, around which the valley is centered, where the spin degeneracy is absent[16,17]. Due to the spin-orbit splitting of the bands at the center of the valley at the K point, the charge carriers with opposite spins are characterized by different effective masses, determined by the second derivatives of the band energy with respect to the crystal momentum[37,38].

The binding energies for A and B dipolar excitons in different TMDC double layers, formed by the same monolayers, are represented in Table II. The highest binding energy corresponds to a $MoSe_2$ double layer, while the lowest corresponds to a WS_2 double layer.

For the double layer heterostructure, formed by two different TNDC monolayers, if the transition metal atom is replaced with another transition metal atom (e.g. for a MoS_2/WS_2 heterostructure) or if the chalcogenide atoms are replaced with the other chalcogenide atoms (e.g. for a $MoS_2/MoSe_2$ heterostructure), we estimated the polarizability as the average of the polarizabilities of two TMDC monolayers. The binding energies for A and B dipolar excitons in different TMDC double layers, formed by two different monolayers, are represented in Tables III and IV, respectively. The highest binding energy corresponds to a double layer with electrons in a $MoSe_2$ monolayer and holes in a MoS_2 monolayer.

TABLE II: Binding energy in eV for A and B type dipolar excitons in a TMDC double layer with the same TMDC materials

N_L h-BN	Binding energy of A exiton, eV				Binding energy of B exiton, eV			
	MoS_2	$MoSe_2$	WS_2	WSe_2	MoS_2	$MoSe_2$	WS_2	WSe_2
8	0.049	0.054	0.040	0.041	0.045	0.050	0.029	0.030
10	0.045	0.049	0.038	0.040	0.043	0.046	0.028	0.029
12	0.042	0.044	0.036	0.038	0.039	0.042	0.028	0.029

Our calculation of the dipolar exciton binding energy by employing the harmonic oscillator approximation for the Keldysh potential for electron-hole attraction shows that the binding energy for A excitons is greater than for B excitons for the TMDC double layer heterostructure with the same monolayers. The latter is related to the fact that the effective masses of spin-down holes from the valence band are sufficiently larger than the effective masses of spin-up holes due to the strong spin-orbit coupling in the valence band of TMDCs, and the effective masses of spin-up electrons from the conduction band are slightly greater than the effective masses of spin-down electrons. Therefore, the reduced mass μ is larger for A excitons than for B excitons, which results in higher binding energies for A excitons than for B excitons. Let us mention that it is possible to create either electrons or holes in either TMDC monolayer by changing the direction of the electric field perpendicular to the plane of the double layer. Since the effective masses of electrons and holes are different for the same TMDC monolayers, the binding energy for dipolar excitons depends on a choice of a monolayer for electrons and holes, correspondingly. According to Tables III and IV, the binding energies for dipolar excitons with electrons in MoS_2 and $MoSe_2$ and holes in WS_2 and WSe_2 are larger than for dipolar excitons with electrons in WS_2 and WSe_2 and holes in MoS_2 and $MoSe_2$.

The energy spectrum of the center-of-mass of the A (or B) dipolar exciton $\varepsilon_0^{A(B)}(\mathbf{P})$ is given by

$$\varepsilon_0^{A(B)}(\mathbf{P}) = \frac{P^2}{2M_{A(B)}}, \tag{14}$$

where P is a momentum of the center of mass of a dipolar exciton, and the masses of A and B dipolar excitons are given by $M_A = m_{e\uparrow} + m_{h\downarrow}$ and $M_B = m_{e\downarrow} + m_{h\uparrow}$, where $m_{e\uparrow(\downarrow)}$ is the effective mass of spin-up (spin-down) electrons from the conduction band and $m_{h\uparrow(\downarrow)}$ is the effective mass of spin-up (spin-down) holes from the valence band, correspondingly.

III. EXCITON-EXCITON INTERACTION

We consider a dilute system of electrons and holes in two parallel TMDC monolayers, spatially separated by a dielectric, when $nr_X^2 \ll 1$, where n is the 2D concentration for dipolar excitons. In this case, the dipolar excitons are formed by electron-hole pairs with the electrons and holes spatially separated in two different TMDC monolayers. One can estimate the concentration of excitons n that corresponds to r_X^{-2} by using Eq. (11). r_X^2 depends on the interlayer separation and when D increases r_X^2 increases. For all TMDC materials r_X^2 varies from 7.4×10^{-18} cm^2 to 9.1×10^{-18} cm^2 that corresponds to the 2D concentrations 1.4×10^{17} cm^{-2} and 1.1×10^{17} cm^{-2} when the interlayer separation is $N_L = 12$ of h-BN monolayers. For the smaller interlayer separation the corresponding concentration even is larger. Below we are considering the dilute limit with the maximal 2D exciton concentration that not exceeded 6×10^{15} cm^{-2}, where the model of a weakly interacting Bose gas is valid.

The excitons, which are not elementary but composite bosons[8] are different from bosons only due to exchange effects[3]. At large interlayer separations D, the exchange effects in the exciton-exciton interactions in a TMDC double

TABLE III: Binding energy in eV for A type dipolar exciton in a TMDC double layer with different TMDC materials

N_L h-BN	Electron layer	MoS_2			$MoSe_2$			WS_2			WSe_2		
	Hole layer	$MoSe_2$	WS_2	WSe_2	MoS_2	WS_2	WSe_2	MoS_2	$MoSe_2$	WSe_2	MoS_2	$MoSe_2$	WS_2
8	B, eV	0.050	0.045	0.047	0.053	0.049	0.050	0.042	0.043	0.045	0.042	0.034	0.046
10	B, eV	0.046	0.043	0.044	0.048	0.045	0.046	0.041	0.041	0.043	0.039	0.033	0.044
12	B, eV	0.042	0.039	0.040	0.044	0.042	0.042	0.038	0.038	0.041	0.036	0.032	0.042

TABLE IV: Binding energy in eV for B type dipolar exciton in a TMDC double layer with different TMDC materials

N_L h-BN	Electron layer	MoS_2			$MoSe_2$			WS_2			WSe_2		
	Hole layer	$MoSe_2$	WS_2	WSe_2	MoS_2	WS_2	WSe_2	MoS_2	$MoSe_2$	WSe_2	MoS_2	$MoSe_2$	WS_2
8	B, eV	0.046	0.038	0.038	0.049	0.041	0.041	0.035	0.035	0.031	0.034	0.027	0.034
10	B, eV	0.043	0.037	0.037	0.045	0.039	0.039	0.034	0.035	0.033	0.033	0.027	0.035
12	B, eV	0.040	0.035	0.035	0.041	0.037	0.037	0.033	0.034	0.032	0.032	0.026	0.034

layer are negligible, because the exchange interactions in a system of spatially separated electrons and holes in a double layer are suppressed due to the low tunneling probability, caused by shielding of the dipole-dipole interaction by the insulating barrier[22]. Therefore, the dilute system of dipolar excitons in a TMDC double layer can be treated as a weakly interacting Bose gas.

The experimental observation by pump-probe spectroscopy[39] of a two-component system of co-existing A and B excitons in a monolayer of MoS_2 was reported. Co-existing A and B excitons can be created employing non-resonant pumping by a broadband laser pulse. In this case, the laser photon energy is much higher than the exciton binding energies. Then created hot free carriers lose energy to phonons and eventually form A and B excitons. The number of A or B excitons is determined by the branching ratios for the various relaxation processes. Since the binding energies for A excitons are larger than for B excitons, the life-time of A excitons is expected to be larger than for B excitons. We consider the system either at the time scales less than the life-tome of B excitons or at the continuous pumping, which will keep creating both types of excitons, substituting recombined excitons.

Assuming that at $T = 0$ K almost all dipolar excitons belong to a BEC, this two-component weakly interacting Bose gas of A and B dipolar excitons can be treated in the framework of the Bogoliubov approximation[40,41]. Within the Bogoliubov approximation for a weakly interacting Bose gas, the many-particle Hamiltonian can be diagonalized, replacing the product of four operators in the interaction term by the product of two operators. This is valid if most of the particles belong to the BEC, and only the interactions between the condensate and non-condensate particles are considered, while the interactions between non-condensate particles are neglected. The operators for condensate bosons are replaced by numbers[40], and the resulting Hamiltonian is quadratic with respect to the creation and annihilation operators.

Let us consider and present the expressions for the coupling constant g for the both Keldysh and Coulomb potentials for interaction between the charge carriers. When two dipolar excitons are separated by the distance R and the electron and hole of one dipolar exciton interact with the electron and hole of another dipolar exciton, then the exciton-exciton interaction potential $U(R)$ can be presented as

$$U(R) = 2V(R) - 2V\left(R\sqrt{1+\frac{D^2}{R^2}}\right), \tag{15}$$

where $V(R)$ is the potential for interaction between two electrons or two holes in the same TMDC monolayer. The interaction $V(R)$ can be given either by the Keldysh potential (2) or by the Coulomb potential.

In a very dilute weakly-interacting Bose gas of dipolar excitons, implying $D \ll R$, the second term in Eq. (15) can be expanded in terms of $(D/R)^2$, and by retaining only the first order terms with respect to $(D/R)^2$, one gets

$$U(R) = \begin{cases} \frac{\pi k e^2 D^2}{2\varepsilon_d \rho_0^2 R}\left[Y_{-1}\left(\frac{R}{\rho_0}\right) - H_{-1}(y)\left(\frac{R}{\rho_0}\right)\right], & \text{for the Keldysh potential,} \\ \frac{k e^2 D^2}{\varepsilon_d R^3}, & \text{for the Coulomb potential.} \end{cases} \tag{16}$$

According to the procedure presented in Ref. [22,42], the exciton-exciton coupling constant g in a very dilute Bose gas of A and B excitons can be obtained under the assumption that the dipole-dipole repulsion of dipolar excitons exists only at distances between excitons larger than the distance from the exciton to the classical turning point. The separation between two dipolar excitons cannot be smaller than this distance, and the coupling constants for the exciton-exciton interaction is obtained as

$$g_i = 2\pi \int_{R_{0i}}^{\infty} RdR\, U(R), \quad i = AA,\ BB,\ AB, \tag{17}$$

where R_{0AA}, R_{0BB}, and R_{0AB} are the distances between two dipolar excitons at the classical turning point for two A excitons, two B excitons, and one A and one B excitons, correspondingly.

Substituting Eq. (16) into Eq. (17), the exciton-exciton coupling constant g can be written as following

$$g_i = \begin{cases} \frac{\pi^2 k e^2 D^2}{\varepsilon_d \rho_0} \left[H_0\left(\frac{R_{0i}}{\rho_0}\right) - Y_0\left(\frac{R_{0i}}{\rho_0}\right) \right], & \text{for the Keldysh potential,} \\ \frac{2\pi k e^2 D^2}{\varepsilon_d R_{0i}}, & \text{for the Coulomb potential.} \end{cases} \tag{18}$$

The system of equations for R_{0AA}, R_{0BB}, and R_{0AB} is derived in Appendix A. The system of equations (A6) has all real and positive roots only if $y_{AA} = y_{BB} = y_{AB} \equiv y$, which implies $R_{0AA} = R_{0BB} = R_{0AB} \equiv R_0$ and $g_{AA} = g_{BB} = g_{AB} \equiv g$. In a very dilute system, the exciton-exciton coupling constant is the same for all three possible combinations of A and B excitons, because at large distances within the dipole approximation (15) the exciton-exciton interaction potential $U(R)$, given by Eq. (16), depends only on the charges of electrons and holes, which are the same for A and B dipolar excitons. Combining Eqs. (A4), (16) and (18), for the Keldysh potential one obtains the following transcendental equation for R_0:

$$4\pi n \rho_0^2 y \left[H_0(y) - Y_0(y) \right] = - \left[H_{-1}(y) - Y_{-1}(y) \right], \tag{19}$$

where $y = R_0/\rho_0$.

For the Coulomb potential one combines Eqs. (A4), (16), (18), implies $R_{0AA} = R_{0BB} = R_{0AB} \equiv R_0$ and derives the following expression for R_0:

$$R_0 = \frac{1}{2\sqrt{\pi n}}. \tag{20}$$

From Eqs. (20), (18) and (A1), we derive the exciton-exciton coupling constant g for the Coulomb potential

$$g = \frac{4\pi k e^2 D^2 \sqrt{\pi n}}{\varepsilon_d}. \tag{21}$$

From Eq. (19) it follows that for the Keldysh potential R_0 depends on the exciton concentration and the type of TMDC material in the double layer, while for the Coulomb potential R_0 depends only on the excitonic concentration according to Eq. (20). The corresponding dependence is replicated for the exciton-exciton coupling constant g, while the coupling constant has the same dependence on the interlayer separation for the both potentials and is directly proportional to D^2. The coupling constant g and the distance R_0 between two dipolar excitons at the classical turning point for different TMDC double layers as functions of the exciton concentration n for the Keldysh potential are represented in Fig. 2. According to Fig. 2, g increases and R_0 decreases as the exciton concentration n increases. While the values of g and R_0 are close to each other for different TMDC double layers, the largest g and R_0 correspond to a WS_2 double layer, and the smallest g and R_0 correspond to a $MoSe_2$ double layer. According to Fig. 2, the difference between exciton-exciton coupling constants g for different TMDC double layers increases as the exciton

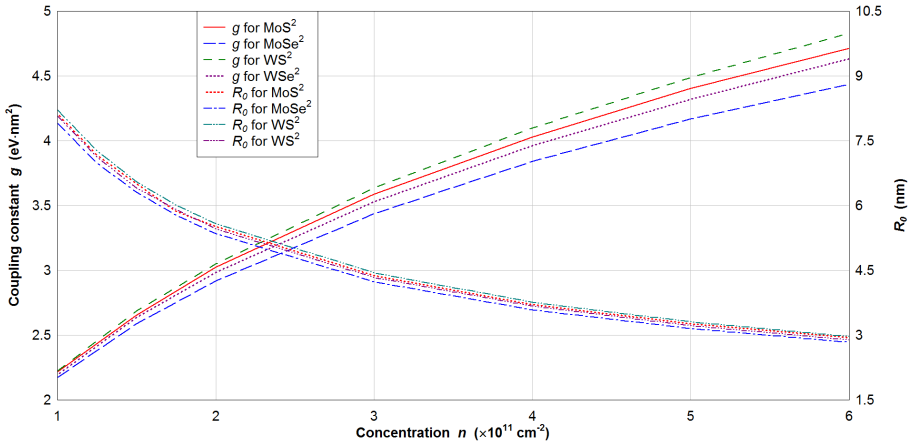

FIG. 2: The coupling constant g and the distance R_0 between two dipolar excitons at the classical turning point for different TMDC double layers as functions of the exciton concentration. The number of h-BN monolayers between the TMDC monolayers is $N_L = 10$. The calculations were performed for the polarizabilities from Ref.[15].

concentration n increases. Since for the Keldysh potential g and R_0 depend on the TMDC material of the double layer only through the polarizability of the material and do not depend on the electrons and holes effective masses, the exciton-exciton coupling constant g does not depend on the choice of the monolayer for either electrons or holes, where the transition metal atom is replaced with the other one and/or the chalcogenide atoms are replaced with the other ones. We did not display g and R_0 for TMDC double layers, formed by the monolayers of different materials, because the results are very close to ones for two monolayers of the same TMDC material, presented in Fig. 2.

The spectrum of collective excitations for a two-component weakly interacting Bose gas of A and B excitons was derived within the Bogoliubov approximation[22]. In the limit of small momenta P, the spectrum of collective excitations has two modes and reads as $\varepsilon_j(P) = c_j P$, where $j = 1, 2$ represents two modes of this spectrum, and c_j are the sound velocities. If the densities of A and B excitons are the same and $n_A = n_B = n/2$, the sound velocity is given by[22]

$$c_j = \sqrt{\frac{gn}{2}\left(\frac{1}{2M_A} + \frac{1}{2M_B} + (-1)^{j-1}\sqrt{\left(\frac{1}{2M_A} - \frac{1}{2M_B}\right)^2 + \frac{1}{M_A M_B}}\right)}. \tag{22}$$

where g is a coupling constant for the interaction between two dipolar excitons, defined above by Eq. (18). Therefore, according to Eq. (22), at $n_A = n_B = n/2$, there is only one non-zero sound velocity $c_S \equiv c_1$ given by

$$c_S = \sqrt{\frac{gn}{2}\left(\frac{1}{M_A} + \frac{1}{M_B}\right)}, \tag{23}$$

while the sound velocity for another mode equals to zero, $c_2 = 0$.

IV. SUPERFLUIDITY

The weakly interacting Bose gas of dipolar excitons in a TMDC double layer satisfies to the Landau criterion for superfluidity[40,41], because at small momenta, the energy spectrum of the quasiparticles is sound-like. The critical exciton velocity for superfluidity is given by $v_c = c_S$, because the quasiparticles can be created only at velocities above the sound velocity.

Within the mean field approximation, the superfluidity in the dilute system of dipolar excitons in a TMDC double layer occurs at the temperatures below the mean field critical temperature of superfluidity T_c, which at $n_A = n_B = n/2$ is given by[22]

$$T_c = \frac{1}{k_B}\left[\frac{\pi\hbar^2 g^2 n^3}{12\zeta(3)}Q\right]^{1/3}. \tag{24}$$

where k_B is the Boltzmann constant, $\zeta(z)$ is the Riemann zeta function ($\zeta(3) \simeq 1.202$), and the factor Q is defined as

$$Q = \frac{M_A + M_B}{(\mu_{AB})^2}. \tag{25}$$

In Eq. (25) $\mu_{AB} = M_A M_B/(M_A + M_B)$ is the reduced mass for two-component system of A and B excitons, M_A and M_B are the effective masses of A and B excitons, correspondingly.

The mean field critical temperature of the superfluidity T_c for the dipolar excitons formed via the Keldysh potential as a function of the exciton concentration n for different TMDC double layers is shown in Fig. 3. According to Fig. 3, T_c increases as n increases. The largest T_c corresponds to a WS_2 double layer, while the smallest T_c corresponds to a $MoSe_2$ double layer, that correlated with the corresponding Q factor presented in Table V. Of course, the mean field critical temperature depends on the polarizability of TMDC material. However, the Q factor has the major impact. Interestingly enough, the corresponding binding energy for the WS_2 is smaller than for the $MoSe_2$. In Fig. 3, we show T_c for the number $N_L = 10$ of h-BN monolayers, located between two TMDC monolayers. The increase of D results in the increase of the potential barrier for electron-hole tunneling between the layers, which leads to the increase of the exciton lifetime. Besides, larger D results in the increase of the exciton dipole moment and the exciton-exciton coupling constant g. Therefore, according to Eq. (23) the sound velocity increases with the increase of g, which leads to the increase of the mean field critical temperature of superfluidity with the increase of D. As it is demonstrated in Fig. 5, T_c increases when D increases.

Let's compare the critical temperatures obtained for the Keldysh and Coulomb potentials. The mean field critical temperature of the superfluidity T_c as a function of the exciton concentration n for WS_2 and $MoSe_2$ double layers for the Keldysh and Coulomb potentials of interaction between the charge carriers is represented in Fig. 4. According to Fig. 4, T_c for the Keldysh potential is smaller than for the Coulomb potential due to the screening effects, taken into account by the Keldysh potential. The screening effects cause the exciton-exciton interaction to become weaker, which leads to smaller exciton-exciton coupling constant g, resulting in smaller T_c.

It is important to mention that while for the Coulomb potential T_c depends on the TMDC materials, forming a double layer, only through the effective exciton masses, constituting the factor Q, for the Keldysh potential T_c depends on the TMDC materials also through the exciton-exciton coupling constant g, determined by the polarizability of the TMDC materials.

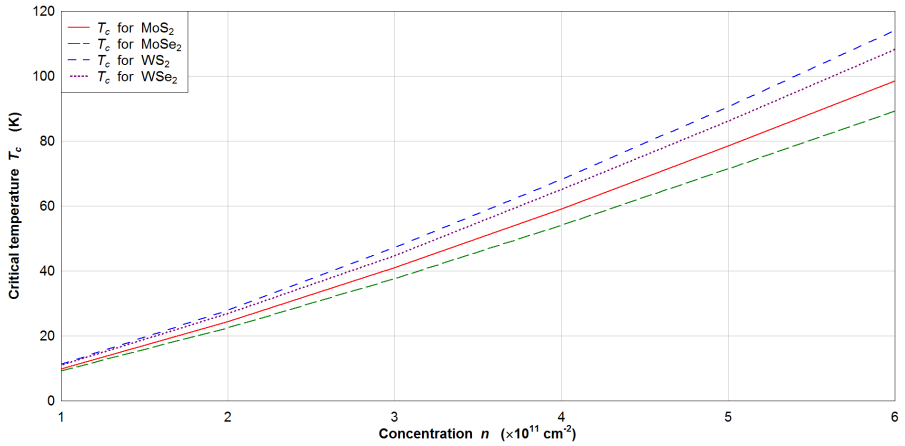

FIG. 3: The mean field critical temperature of the superfluidity T_c as a function of the exciton concentration n for different TMDC double layers. The calculations were performed for the number $N_L = 10$ of h-BN monolayers, located between two TMDC monolayers, The calculations were performed for the polarizabilities from Ref.[15] and the set of effective masses for electrons and holes from Refs.[37,38].

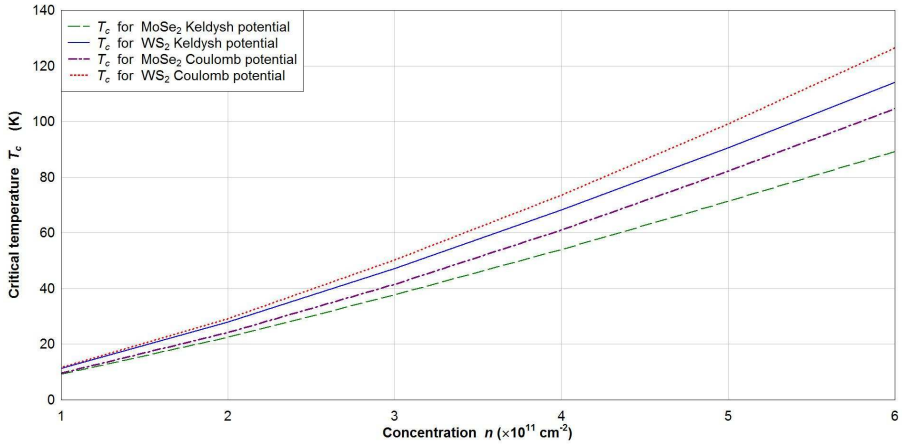

FIG. 4: The mean field critical temperature of the superfluidity T_c as a function of the exciton concentration n for WS_2 and $MoSe_2$ double layers for the Keldysh and Coulomb potentials of interaction between the charge carriers. The calculations were performed for the number $N_L = 10$ of h-BN monolayers, located between two TMDC monolayers. The calculations were performed for the polarizabilities from Ref.[15] and the set of effective masses for electrons and holes from Refs.[37,38].

The mean field critical temperature of the superfluidity T_c for a WS_2 double layer under the assumption about the Coulomb potential for the interaction between the charge carriers is represented as a function of the exciton concentration n and the interlayer separation D in Fig. 5. We choose to plot T_c for a WS_2 double layer, since T_c for this material is larger than for other materials at the same n and D. According to Fig. 5, T_c increases as n and D increase.

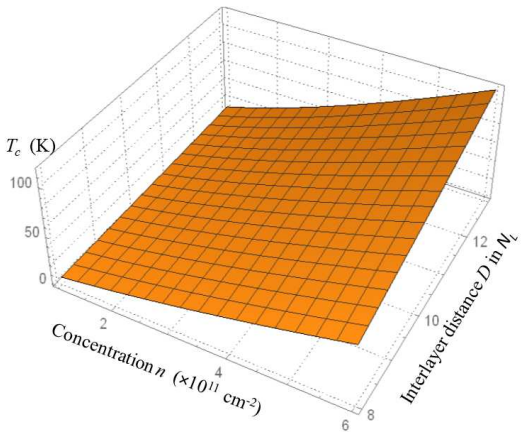

FIG. 5: (Color online) The mean field critical temperature of the superfluidity T_c for a WS_2 double layer as a function of the exciton concentration n and the interlayer separation D. The calculations were performed for the set of effective masses for electrons and holes from Refs.[37,38].

TABLE V: Q factor in units of $1/m_0$, reduced mass μ_{AB} and $M_A + M_B$ in units of m_0 for A and B type dipolar excitons in a TMDC double layer with the same TMDC materials

	MoS_2	$MoSe_2$	WS_2	WSe_2
Q, $[1/m_0]$	7.74	6.52	11.47	10.67
μ_{AB}, $[m_0]$	0.52	0.62	0.36	0.39
$M_A + M_B$, $[m_0]$	2.08	2.48	1.46	1.49

Let us mention that while for a one-component Bose gas of particles with the same mass the critical temperature of superfluidity is a decreasing function of the mass of a particle, for a two-component weakly interacting Bose gas of A and B dipolar excitons T_c is an increasing function of the factor Q according to Eq. (24), where the dependence of the factor Q on the effective masses of A and B dipolar excitons is given by Eq. (25). The factors Q for A and B type excitons in different TMDC double layers, formed by two monolayers of the same material, are presented in Table V. The factors Q for A and B type excitons in different TMDC double layers, formed by two monolayers of two different materials, when the transition metal atom is replaced by the other transition metal atom (e.g. for a MoS_2/WS_2 heterostructure) or when the chalcogenide atoms are replaced by the other chalcogenide atoms (e.g. for a $MoS_2/MoSe_2$ heterostructure), are presented in Table VI. According to Tables V and VI, the largest factor Q corresponds to a double layer, formed by two WS_2 monolayers, while the smallest factor Q corresponds to a double layer, formed by two $MoSe_2$ monolayers. The critical temperature of superfluidity T_c in different combinations of TMDC double layers for different densities and corresponding Q factor are shown in Table VII. Since the effective masses of electrons and holes are different for the same TMDC monolayers, the factor Q and T_c depend on a choice of a monolayer for electrons and holes, correspondingly. According to Table VII, for a given TMDC double layer there is a correlation between Q and T_c, implying that higher T_c corresponds to the double layer with higher Q, as follows from Eq. (24). As it can be seen in Table VII, the largest T_c and Q correspond to a double layer, formed by two WS_2 monolayers, while the smallest T_c and Q correspond to a double layer, formed by two $MoSe_2$ monolayers.

Applying Eqs. (24) and (25) to dipolar excitons with mass M in semiconductor (GaAs/AlGaAs) coupled quantum wells, we substitute $M \equiv M_A = M_B$ and divide the exciton concentration n on the spin degeneracy factor $g_s = 4$, which is caused by the spin degeneracy of electrons and holes, forming an exciton in semiconductor coupled quantum wells. In this case, the factor $Q^{1/3}n$ in Eq. (24) will be replaced by $n/(2M^{1/3})$. This estimation as well as the possibility of using for the dielectric barrier h-BN monolayers with smaller dielectric constant 4.89 than the dielectric constant 13 for GaAs result in higher T_c for dipolar excitons in a TMDC double layer than for semiconductor coupled quantum wells. The dependence of the critical temperature on the spin degeneracy factor was shown in Refs. 43,44. We do not divide n on g_s for the excitons in a TMDC double layer due to the absence of the spin degeneracy in TMDC monolayers around the K point in the Brillouin zone[16,17].

V. CONCLUSIONS

In this paper we have studied the formation and superfluidity of dipolar excitons in double layer heterostructures that are formed by two monolayers of the same TMDC material and two different TMDC monolayers. In the framework of the harmonic oscillator approximation for the Keldysh potential the analytical expressions for the exciton energy spectrum and the mean field critical temperature of superfluidity are obtained. All calculations are performed by using the effective electron and hole masses and polarizability obtained within the framework of DFT approach for the TMDC material. We have calculated the binding energies for A and B dipolar excitons in various TMDC double layers, taking into account screening effects by employing the approximated Keldysh potential for the interaction between the charge carriers. The binding energy of dipolar excitons depends on the electron and hole reduced mass, the polarizability of the TMDC material and the interlayer separation between two monolayers. Since the effective masses of electrons and holes are different for the same TMDC monolayers, the exciton binding energy is larger for dipolar excitons with electrons in MoS_2 and $MoSe_2$ and holes in WS_2 and WSe_2 than for dipolar excitons with electrons in WS_2 and WSe_2 and holes in MoS_2 and $MoSe_2$. The increase of the electron and hole reduced mass leads to the decrease of the binding energy of dipolar exciton. The mean field critical temperature of superfluidity T_c for a dilute system of A and B dipolar excitons in TMDC materials are determined by the exciton-exciton coupling constant g and the factor Q, which depends of the sum of the effective masses of A and B excitons and the reduced mass for a two-component system of A and B excitons. Different effective electron and hole masses result in different effective masses of A and B excitons M_A and M_B, a different reduced mass μ_{AB} for two-component system of A and B excitons, and a different factor Q. We have calculated the exciton-exciton coupling constant g and the mean field critical temperature superfluidity T_c for a dilute two-component system of A and B dipolar excitons. Let us mention that T_c for a two-component weakly interacting gas of A and B dipolar excitons is an increasing function of the factor Q, determined by the effective reduced mass of A and B excitons, which is always smaller than the individual effective mass of either A or B exciton. While the factor Q and T_c depend on the exciton effective masses, the exciton-exciton coupling constant g and the distance between two dipolar excitons at the classical turning point R_0 do not depend on the exciton effective masses but depend on the exciton concentration and the polarizability of TMDC materials. The critical temperature of superfluidity T_c, calculated by using the harmonic potential approximation of the Keldysh potential for the interaction between the charge carriers, is smaller than for the Coulomb potential due to diminishing exciton-exciton interaction by screening effects, taken into account by the Keldysh potential. These screening effects lead to the decrease of the exciton-exciton coupling constant, which results in the decrease of T_c. The largest mean field critical temperature T_c of two-component superfluidity of A and B dipolar excitons was obtained for a WS_2 double layer, while the smallest T_c was obtained for a $MoSe_2$ double layer. For a given 2D exciton concentration n and interlayer separation D, the TMDC double layer with higher T_c corresponds to the double layer with higher Q. By comparison of the exciton-exciton coupling g and the mean field critical temperature T_c of superfluidity calculated by using the Keldysh and Coulomb potential for the interaction between the charge carriers, one can study the influence of the screening effects on a weakly interacting gas of dipolar excitons in a TMDC double layer.

Appendix A: Interactions in a two-component weakly interacting gas of A and B dipolar excitons

In this appendix, we analyze the interactions in a two-component weakly interacting gas of A and B dipolar excitons and derive the system of equations for R_{0i}.

The chemical potentials μ_A and μ_B for A and B excitons, respectively, of the weakly interacting Bose gas of dipolar excitons within the Bogoliubov approximation are represented as[22]

$$\mu_A - \mathcal{A}_A = g_{AA}n_A + g_{AB}n_B,$$

TABLE VI: Q factor in units of $1/m_0$, reduced mass μ_{AB} and $M_A + M_B$ in units of m_0 for A and B type dipolar excitons in a TMDC double layer with different TMDC materials

Electron layer	MoS_2			$MoSe_2$			WS_2			WSe_2		
Hole layer	$MoSe_2$	WS_2	WSe_2	MoS_2	WS_2	WSe_2	MoS_2	$MoSe_2$	WSe_2	MoS_2	$MoSe_2$	WS_2
Q, $[1/m_0]$	7.31	9.25	9.05	6.86	8.03	7.88	9.17	8.57	11.2	8.80	8.25	10.9
μ_{AB}, $[m_0]$	0.55	0.44	0.45	0.59	0.50	0.52	0.44	0.47	0.37	0.46	0.49	0.38
$M_A + M_B$, $[m_0]$	2.21	1.77	1.82	2.35	2.04	2.09	1.77	1.90	1.51	1.85	1.98	1.54

TABLE VII: Critical temperature of superfluidity T_c in K in different combinations of TMDC double layers for diffident densities and the number $N_L = 10$ of h-BN monolayers, located between two TMDC monolayers, and corresponding Q factor in units of $1/m_0$

Electron layer	MoS_2				$MoSe_2$				WS_2				WSe_2			
Hole layer	MoS_2	$MoSe_2$	WS_2	WSe_2	MoS_2	$MoSe_2$	WS_2	WSe_2	MoS_2	$MoSe_2$	WS_2	WSe_2	MoS_2	$MoSe_2$	WS_2	WSe_2
$n = 3\times10^{11}$ cm^{-2}	41	39	44	43	40	38	41	40	43	42	47	47	43	41	46	45
$n = 5\times10^{11}$ cm^{-2}	79	76	84	82	77	71	79	77	83	80	91	89	81	78	88	86
Q, $[1/m_0]$	7.74	7.31	9.25	9.05	7.54	6.52	8.03	7.88	9.17	8.57	11.47	11.2	8.80	8.25	10.9	10.67

$$\mu_B - \mathcal{A}_B = g_{BB}n_B + g_{AB}n_A, \tag{A1}$$

where $n_{A(B)}$ is the concentration for A(B) dipolar excitons, $g_{AA(BB)}$ and g_{AB} are the exciton-exciton coupling constants for the interaction between two A dipolar excitons, two B dipolar excitons and for the interaction between A and B dipolar excitons, respectively, $\mathcal{A}_A$ and $\mathcal{A}_B$ are the constants, determined by A and B dipolar exciton binding energy, correspondingly, and the gap, formed by a spin-orbit coupling for the A (B) dipolar exciton[22]. One can obtain from Eq. (A1) the following equation:

$$\mu_A + \mu_B - \mathcal{A}_A - \mathcal{A}_B = g_{AA}n_A + g_{BB}n_B + g_{AB}n, \tag{A2}$$

where $n = n_A + n_B$ is the total 2D concentration of excitons.

Below we present the expressions for the coupling constant g for the both Keldysh and Coulomb potentials for the interaction between the charge carriers.

According to the procedure presented in Refs. [22,42], two dipolar excitons cannot be closer to each other than at the distance R_{0i}, which is determined by the condition, following from the fact that the energy of two dipolar excitons cannot exceed the doubled chemical potential μ of the system, i.e.[22],

$$2\mathcal{A}_A + U(R_{0AA}) = 2\mu_A, \qquad 2\mathcal{A}_B + U(R_{0BB}) = 2\mu_B\ , \qquad \mathcal{A}_A + \mathcal{A}_B + U(R_{0AB}) = \mu_A + \mu_B, \tag{A3}$$

where $U(R)$ is the potential of interaction between the dipolar excitons separated at the distance R. Using Eqs. (A1), (A2), and (A3), one obtains

$$\begin{aligned} \frac{U(R_{0AA})}{2} &= g_{AA}n_A + g_{AB}n_B, \\ \frac{U(R_{0BB})}{2} &= g_{BB}n_B + g_{AB}n_A, \\ U(R_{0AB}) &= g_{AA}n_A + g_{BB}n_B + g_{AB}n. \end{aligned} \tag{A4}$$

Let us mention that the third equation in Eq. (A4) can be replaced by the following:

$$U(R_{0AB}) = \frac{1}{2}\left(U(R_{0AA}) + U(R_{0BB})\right). \tag{A5}$$

Then the system of the equations (A4) can be formed by the first and the second equations from Eq. (A4) and Eq. (A5).

Substituting Eqs. (16) and (18) into Eq. (A4), one obtains the following system of three equations for R_{0i} for the Keldysh potential:

$$\begin{aligned} &4\pi\rho_0^2 y_{AA}\left[n_A\left[H_0\left(y_{AA}\right) - Y_0\left(y_{AA}\right)\right] + n_B\left[H_0\left(y_{AB}\right) - Y_0\left(y_{AB}\right)\right]\right] = -\left[H_{-1}\left(y_{AA}\right) - Y_{-1}\left(y_{AA}\right)\right], \\ &4\pi\rho_0^2 y_{BB}\left[n_B\left[H_0\left(y_{BB}\right) - Y_0\left(y_{BB}\right)\right] + n_A\left[H_0\left(y_{AB}\right) - Y_0\left(y_{AB}\right)\right]\right] = -\left[H_{-1}\left(y_{BB}\right) - Y_{-1}\left(y_{BB}\right)\right], \\ &2\pi\rho_0^2 y_{AB}\left[n_A\left[H_0\left(y_{AA}\right) - Y_0\left(y_{AA}\right)\right] + n_B\left[H_0\left(y_{BB}\right) - Y_0\left(y_{BB}\right)\right] + n\left[H_0\left(y_{AB}\right) - Y_0\left(y_{AB}\right)\right]\right] \\ =\ &-\left[H_{-1}\left(y_{AB}\right) - Y_{-1}\left(y_{AB}\right)\right], \end{aligned} \tag{A6}$$

where $y_i = R_{0i}/\rho_0$.

If the densities of A and B excitons are the same and $n_A = n_B = n/2$, Eqs. (A6) result in the following system of equations

$$\begin{aligned} &2\pi n\rho_0^2 y_{AA}\left[H_0\left(y_{AA}\right) - Y_0\left(y_{AA}\right) + H_0\left(y_{AB}\right) - Y_0\left(y_{AB}\right)\right] = -\left[H_{-1}\left(y_{AA}\right) - Y_{-1}\left(y_{AA}\right)\right], \\ &2\pi n\rho_0^2 y_{BB}\left[H_0\left(y_{BB}\right) - Y_0\left(y_{BB}\right) + H_0\left(y_{AB}\right) - Y_0\left(y_{AB}\right)\right] = -\left[H_{-1}\left(y_{BB}\right) - Y_{-1}\left(y_{BB}\right)\right], \\ &\pi n\rho_0^2 y_{AB}\left[H_0\left(y_{AA}\right) - Y_0\left(y_{AA}\right) + H_0\left(y_{BB}\right) - Y_0\left(y_{BB}\right) + 2H_0\left(y_{AB}\right) - 2Y_0\left(y_{AB}\right)\right] \\ =\ &-\left[H_{-1}\left(y_{AB}\right) - Y_{-1}\left(y_{AB}\right)\right]. \end{aligned} \tag{A7}$$

Substituting Eqs. (16) into Eq. (A5), one can replace the third equation in Eqs. (A6) by the following equation:

$$\frac{1}{y_{AB}}\left[Y_{-1}\left(y_{AB}\right)-H_{-1}\left(y_{AB}\right)\right]=\frac{1}{2y_{AA}}\left[Y_{-1}\left(y_{AA}\right)-H_{-1}(y)\left(y_{AA}\right)\right]+\frac{1}{2y_{BB}}\left[Y_{-1}\left(y_{BB}\right)-H_{-1}(y)\left(y_{BB}\right)\right]. \quad \text{(A8)}$$

[1] L. Pitaevskii and S. Stringari, *Bose-Einstein Condensation* (Clarendon Press, Oxford, 2003).
[2] F. Daflovo, S. Giorgini, and L. P. Pitaevskii, Rev. Mod. Phys. **71**, 463 (1999).
[3] S. A. Moskalenko and D. W. Snoke, *Bose-Einstein Condensation of Excitons and Biexcitons and Coherent Nonlinear Optics with Excitons* (Cambridge University Press, New York, 2000).
[4] Yu. E. Lozovik and V. I. Yudson, Zh. Eksp. Teor. Fiz. **71**, 738 (1976) [Sov. Phys. JETP **44**, 389 (1976)]; Physica A **93**, 493 (1978).
[5] R. Anankine, M. Beian, S. Dang, M. Alloing, E. Cambril, K. Merghem, C. G. Carbonell, A. Lematre, and F. Dubin, Phys. Rev. Lett. **118**, 127402 (2017).
[6] L. V. Butov, J. Phys.: Condens. Matter **16**, R1577 (2004).
[7] D. W. Snoke, "Dipole excitons in coupled quantum wells: toward an equilibrium exciton condensate," in Quantum Gases: Finite Temperature and Non-Equilibrium Dynamics (Vol. 1, Cold Atoms Series), N.P. Proukakis, S.A. Gardiner, M.J. Davis, and M.H. Szymanska, eds. (Imperial College Press, London, 2013).
[8] M. Combescot, R. Combescot, and F. Dubin, Rep. Prog. Phys. **80**, 066501 (2017).
[9] A. Kormányos, G. Burkard, M. Gmitra, J. Fabian, V. Zólyomi, N. D. Drummond, and V. Fal'ko, 2D Mater. **2**, 022001 (2015).
[10] K. F. Mak, C. Lee, J. Hone, J. Shan, and T. F. Heinz, Phys. Rev. Lett. **105**, 136805 (2010).
[11] K. F. Mak, K. He, J. Shan, and T. F. Heinz, Nat. Nanotechnol. **7**, 494 (2012).
[12] L. Britnell, R. M. Ribeiro, A. Eckmann, R. Jalil, B. D. Belle, A. Mishchenko, Y.-J. Kim, R. V. Gorbachev, T. Georgiou, S. V. Morozov, A. N. Grigorenko, A. K. Geim, C. Casiraghi, A. H. Castro Neto, and K. S. Novoselov, Science **340**, 1311 (2013).
[13] W. Zhao, Z. Ghorannevis, L. Chu, M. Toh, C. Kloc, P.-H. Tan, and G. Eda, ACS Nano **7**, 791 (2013).
[14] A. Chernikov, T. C. Berkelbach, H. M. Hill, A. Rigosi, Y. Li, O. B. Aslan, D. R. Reichman, M. S. Hybertsen, and T. F. Heinz, Phys. Rev. Lett. **113**, 076802 (2014).
[15] T. C. Berkelbach, M. S. Hybertsen, and D. R. Reichman, Phys. Rev. B **88**, 045318 (2013).
[16] A. F. Morpurgo, Nat. Phys. **9**, 532 (2013).
[17] S. Fang, R. K. Defo, S. N. Shirodkar, S. Lieu, G. A. Tritsaris, and E. Kaxiras, Phys. Rev. B **92**, 205108 (2015).
[18] M. M. Fogler, L. V. Butov, and K. S. Novoselov, Nature Commun. **5**, 4555 (2014).
[19] F. Ceballos, M. Z. Bellus, H.-Y. Chiu, and H. Zhao, ACS Nano **8**, 12717 (2014).
[20] E. V. Calman, C. J. Dorow, M. M. Fogler, L. V. Butov, S. Hu, A. Mishchenko, and A. K. Geim, Appl. Phys. Lett. **108**, 101901 (2016).
[21] F.-C. Wu, F. Xue, and A. H. MacDonald, Phys. Rev. B **92**, 165121 (2015).
[22] O. L. Berman and R. Ya. Kezerashvili, Phys. Rev. B **93**, 245410 (2016).
[23] L. D. Landau and E. M. Lifshitz, *Quantum Mechanics: Non Relativistic Theory* (Addison-Wesley, Reading, MA, 1958).
[24] E. Prada, J. V. Alvarez, K.'L. Narasimha-Acharya, F. J. Bailen, and J. J. Palacios, Phys. Rev. B **91**, 245421 (2015).
[25] K.'A. Velizhanin and A. Saxena, Phys. Rev. B **92**, 195305 (2015).
[26] D.K. Zhang, D.W. Kidd, and K. Varga, Phys. Rev. B **93**, 125423 (2016)
[27] R.Ya. Kezerashvili and Sh. M. Tsiklauri, Few-Body Syst. **58**, 18 (2017).
[28] L. V. Keldysh, Zh. Eksp. Teor. Fiz. Pis. Red. **29**, 716 (1979) [JETP Lett. **29**, 658 (1979)].
[29] P. Cudazzo, I. V. Tokatly, and A. Rubio, Phys. Rev. B **84**, 085406 (2011).
[30] A. S. Rodin, A. Carvalho, and A. H. Castro Neto, Phys. Rev. B **90**, 075429 (2014).
[31] Y. Cai, L. Zhang, Q. Zeng, L. Cheng, and Y. Xu, Solid State Commun. **141**, 262 (2007).
[32] V. Fock, Z. Phys. **47**, 446 (1928).
[33] C. G. Darwin, Proc. Cambridge Philos. Soc. **27**, 86 (1930).
[34] R. B. Dingle, Proc. Roy. Soc. London A **211**, 500 (1952).
[35] P. A. Maksym and T. Chakraborty, Phys. Rev. Lett. **65**, 108 (1990).
[36] A. Iyengar, J. Wang, H. A. Fertig, and L. Brey, Phys. Rev. B **75**, 125430 (2007).
[37] A. Kormanyos, V. Zolyomi, N. D. Drummond, and G. Burkard, Phys. Rev. X **4**, 011034 (2014).
[38] I. Kylänpää and H.-P. Komsa, Phys. Rev. B **92**, 205418 (2015).
[39] C. Mai, A. Barrette, Y. Yu, Yu. G. Semenov, K. W. Kim, L. Cao, and K. Gundogdu, Nano Lett. **14**, 202 (2014).
[40] A. A. Abrikosov, L. P. Gorkov, and I. E. Dzyaloshinskii, *Methods of Quantum Field Theory in Statistical Physics*(Prentice-Hall, Englewood Cliffs, NJ, 1963).
[41] E. M. Lifshitz and L. P. Pitaevskii, *Statistical Physics, Part 2* (Pergamon Press, Oxford, 1980).
[42] O. L. Berman, R. Ya. Kezerashvili, G. V. Kolmakov, and Yu. E. Lozovik, Phys. Rev. B **86**, 045108 (2012).
[43] A. L. Ivanov, P. B. Littlewood, and H. Haug, Phys. Rev. B **59**, 5032 (1999).
[44] L. V. Butov, A. C. Gossard, and D. S. Chemla, Nature (London) **418**, 751 (2002).